buildings

MDPI

Article

An Experimental Study of Granular Material Using Recycled Concrete Waste for Pavement Roadbed Construction

Hasan Al-Mosawe [1], Amjad Albayati [2], Yu Wang [3] and Nuha S. Mashaan [4,*]

[1] Civil Engineering Department, College of Engineering, Al-Nahrain University, Baghdad 10071, Iraq
[2] Civil Engineering Department, College of Engineering, University of Baghdad, Baghdad 10071, Iraq
[3] School of Science, Engineering and Environment, University of Salford, Manchester M50 2EQ, UK
[4] Faculty of Science and Engineering, School of Civil and Mechanical Engineering, Curtin University, Bentley, WA 6102, Australia
* Correspondence: nuhas.mashaan1@curtin.edu.au

Abstract: Rapid worldwide urbanization and drastic population growth have increased the demand for new road construction, which will cause a substantial amount of natural resources such as aggregates to be consumed. The use of recycled concrete aggregate could be one of the possible ways to offset the aggregate shortage problem and reduce environmental pollution. This paper reports an experimental study of unbound granular material using recycled concrete aggregate for pavement subbase construction. Five percentages of recycled concrete aggregate obtained from two different sources with an originally designed compressive strength of 20–30 MPa as well as 31–40 MPa at three particle size levels, i.e., coarse, fine, and extra fine, were tested for their properties, i.e., the optimum moisture content density, Californian bearing ratio, and resilient modulus. A characterization of the resilient modulus of the mixes under complex stress conditions was performed. The characterized modulus model was used in the nonlinear analysis of the pavement structure under traffic loading using KENALYER software. Consequently, the two critical responses, i.e., the tensile strain at the bottom of the asphalt layer and the vertical compressive strain at the top of the subgrade, were computed and compared for the pavement structures with varying types and percentages of recycled concrete aggregate used in the subbase layer.

Keywords: pavement; recycled concrete aggregate; stiffness; subbase construction

Citation: Al-Mosawe, H.; Albayati, A.; Wang, Y.; Mashaan, N.S. An Experimental Study of Granular Material Using Recycled Concrete Waste for Pavement Roadbed Construction. *Buildings* **2022**, *12*, 1926. https://doi.org/10.3390/buildings12111926

Academic Editor: Jorge de Brito

Received: 15 October 2022
Accepted: 7 November 2022
Published: 8 November 2022

1. Introduction

It is estimated by 2030, 2.59 billion tons of solid waste will be generated annually at a global level. By 2050, this amount is expected to rise further to 3.40 billion tons (Stone Cycling 2021) [1]. The World Bank (2018) [2] estimated that only about 19% of solid waste globally was reused through recycling and composting. Researchers have used different types of waste materials to produce eco-friendly developed construction materials [3–7]. In the EU, construction and demolition waste (CDW) accounts for more than one third of all waste generated. This includes all of the waste produced by the construction and demolition of buildings and infrastructure, as well as road planning and maintenance (European Commission). In the UK, according to the 2020 Defra Statistics report, in 2016, about 66.2 million tons of non-hazardous CDW was generated. Concrete waste is the major contributor of CDW (Tam, 2008) [8], reaching 75% (Arabani and Azarhoosh 2012) [9]. Effectively reducing CDW problems, such as land contamination and air pollution, as well as health and safety is a global challenge to tackle climate change and for sustainable development and the circular economy. CDW recycling for new construction projects has been increasingly adopted in civil engineering practice. The UK governmental statistics show that 91% of non-hazardous CDW is recovered; much of this is concrete, brick, and asphalt (SteelConstruction.info). In general, these recycled materials are primarily used

for aggregates (Marinković 2012) [10]. One of the popular applications is to use the recycled concrete aggregate (RCA) as alternative unbound gravel material for pavement subbase in road construction (Pourkhorshidi et al. 2020) [11,12-14]. Many researchers have investigated the effects of the application (Seferoglu et al. 2018) [15]. A recent study using RCAs obtained from concretes with three different compressive strengths to replace natural aggregates at rates of 25, 50, and 75% recommended blending the RCAs with the natural material rather than to use them in pure form (Toka & Olgun 2021) [16]. RCA has been also studied to work together with geogrid reinforcement. The results showed that in the application, RCA particles had a low rate of breakup at the same particle gradation of the constructed subbase specification (Alnedawi and Rahman 2021) [17]. The use of RCA has attracted researchers, who aim to improve material performance, which contributes to a longer pavement structure design life (Tran et al. 2021; Farhan 2019; Albayati et al. 2018a; Albayati et al. 2018b; Hama et al. 2018) [18-22].

In addition to the bearing capacity and strength, moisture has a considerable influence on the performance of unbound gravel materials and the constructed base course. The increase in the moisture content in the unbound granular material would cause a reduction in the effective stress and would consequently decrease the base course resistance to permanent deformation (Haynes 1961; Barksdale 1972; Fredrick et al. 2000; Abid et al. 2017) [23-26]. An early study (Poon and Chan, 2006) [27] using recycled concrete aggregates and crushed clay brick as aggregates in unbound subbase materials showed that the use of 100% recycled concrete aggregates increased the optimum moisture content but decreased the maximum dry density of the subbase materials. The California bearing ratio for the unsoaked and soaked subbase materials with 100% RCA was lower than that of the materials with natural aggregates.

Aggregate particle grading and the content of fine particles also play an important role in the mechanical properties of granular materials (Dunlap 1966) [28]. Recent research (Thai et al. 2022; Signes et al.) [29,30] investigated the effects of the compaction degree and particle size on the CBR magnitude, showing that strength was enhanced with the compact energy but decreased with the fine particle (<0.075 mm) content. However, so far, the information about the particle size influence on the granular materials using RCA and for the application of pavement base course construction is still limited, particularly regarding the knowledge of the combined effect of the aggregate size and the usage at different ranges of size specification. To contribute more knowledge for the use of RCA in pavement construction, this paper reports a study of the effect of using RCA for the subbase. Two types of RCA were investigated for their usage and size. Three material properties were tested and compared with those of a conventional granular subbase material (CGSM).

2. Experimental Work

2.1. Raw Materials

The two types of RCA were from the CDW of Texas T-wall barriers with an originally designed compressive strength of 20–30 MPa and the CDW of concrete cubes with an originally designed compressive strength of 31–40 MPa. These cubes were obtained from laboratory tests of construction material wastes and were characterized according to the cube compressive strength. Figure 1 shows the two kinds of CDWs. Figure 2 shows the crushed RCA of the two CDWs and the CGSM used for pavement construction.

(**a**) (**b**)

Figure 1. The CDW. (**a**) Texas T-wall barriers (TTB). (**b**) Concrete cubes (CC)

(**a**) (**b**) (**c**)

Figure 2. The RCA and CGSM. (**a**) RCA of TTB. (**b**) RCA of CC. (**c**) CGSM

Figure 3 shows the particle gradation of the CGSM, which is in the range of the speciation limits for the type B soil-aggregate mixture (ASTM D 1241). The physical properties of the coarse particles (≥2 mm) and the fine particles (passed through a 2 mm sieve) of the CGSM and the two types of RCA are listed in Table 1.

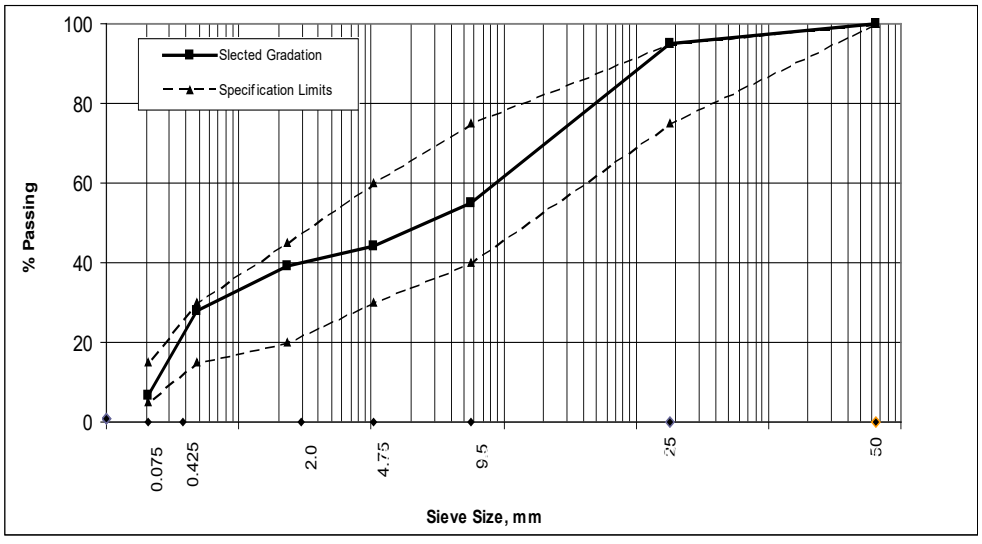

Figure 3. Selected CGSM gradation and specification limit.

Table 1. Physical Properties of the Soil Aggregates.

Property	ASTM Design	Test Results			ASTM D 1241 Specification Limit
		CGSM	TTB RCA	CC RCA	
Coarse aggregates (≥2 mm)					
Bulk specific gravity	C-127	2.631	2.314	2.332	Not limited
Apparent specific gravity		2.634	2.482	2.502	Not limited
Water absorption (%)		0.271	2.98	2.73	Not limited
Percent wear by Los Angeles abrasion (%)	C-131	19	31	27	50 max.
Soundness loss by sodium sulfate solution (%)	C-88	4.1	6.9	6.4	Not limited
Fine aggregates (<2 mm)					
Bulk specific gravity	C-128	2.561	2.092	2.102	Not limited
Apparent specific gravity		2.622	2.223	2.241	Not limited
Water absorption (%)		0.809	4.953	4.303	Not limited
Plasticity index (%)	D2419	Non Plastic	Non Plastic	Non Plastic	Max. 6

The RCA was used to replace the corresponding size of the CGSM for three ranges of particles, i.e., coarse (≥2 mm), fine (2–0.075 mm), and extra fine (<0.075 mm), by 5 different percentages of the weight of the particles in each size range: 0, 25, 50, 75, and 100%. For example, the replacement of 25 percent of the fine aggregates means the replacement of 25% of the weight of the CGSM retained in the sieves between 2 mm and 0.075 mm. For ease of reference, Table 2 shows the classification and nomenclature for mixes designed and tested in this study. For example, RCA30/50 indicates the mix consists of the coarse RCA of TTB of original strength of 20–30 MPa to replace 50% (by weight) of the coarse aggregate of CGSM.

Table 2. Nomenclature and Description of the Mixes.

Replacement Rate %	RCA of TTB			RCA of CC		
	Coarse ≥2 mm	Fine 2–0.075 mm	Extra fine >0.075 Mm	Coarse ≥2 mm	Fine 2–0.075 mm	Extra fine >0.075 mm
0	Control Mix (CM)					
25	TTB_RCA/25	TTB_RFA/25	TTB_EFA/25	CC_RCA/25	CC_RFA/25	CC_REF/25
50	TTB_RCA/50	TTB_RFA/50	TTB_EFA/50	CC_RCA/50	CC_RFA/50	CC_REF/50
75	TTB_RCA/75	TTB_RFA/75	TTB_EFA/75	CC_RCA/75	CC_RFA/75	CC_REF/75
100	TTB_RCA/100	TTB_RFA/100	TTB_EFA/100	CC_RCA/100	CC_RFA/100	CC_REF/100

3. Experimental Tests

A total of three laboratory tests were performed for the mixes in Table 2: moisture–density test for the compaction property, CBR test for the bearing property or strength, and resilient modulus test for stiffness.

3.1. Mositure–Density Test

The moisture content will influence the compact ability of granular materials. It has a lubricating function due to the water at the particles' interface and a resistance to compaction due to its own volume of bulk water retained in the pore spaces. It directly

influences the density/porosity of the final state of compaction. There is an optimum moisture content for the sake of compaction, at which the maximum density or the minimum porosity may be reached. To determine the optimum moisture content and the corresponding maximum density of compacted mixes, a modified proctor test was carried out according to ASTM D 1557.

The prepared granular mixtures of a certain water content were loaded into a cylindrical mold. The mold sizes were 152.4 mm in diameter and 116.5 mm in height, of which 50.8 mm acted as a collar extension. Mixes were loaded into the mold in five layers. After the addition of each layer, the mixes were compacted by 56 blows using a 44.5 N (10 lbf) rammer dropped from a height of 457 mm (18 in.) to produce a total compaction force of about 2700 kN·m/m^3 (56,000 ft·lbf/ft^3). After compaction, the mixtures were weighed and their density calculated. In total, five water contents were tested.

3.2. California Bearing Ratio (CBR) test

The CBR test is used as a measurement for the bearing capacity of granular materials. A benchmark using a well-graded crushed stone particles is set as the reference of 100% CBR magnitude. The CBR test was conducted following ASTM D1883. All sample mixes were prepared to their optimum moisture content. They were loaded into molds of 150 mm diameter in five different layers and were compacted after each layer was added following the identical procedure described before for the moisture–density test. After compaction, samples were kept in molds and immersed in water for a period of 96 h. During this period, a 4.5 kg surcharge weight was applied on the top of the samples. The CBR test involves applying a vertical penetrating load using a small piston at a rate of 1.3 mm (0.05 in.) per minute and recording the loads and penetration depths at the range from 0.64 mm (0.025 in.) to 7.62 mm. From the test curve, the applied forces corresponding to the penetration were read. The CBR value was the highest load in the penetration range from 2.5 mm to 5 mm. Figure 4 shows the specimen under compaction and CBR testing.

(**a**) (**b**)

Figure 4. The CBR test. (**a**) Specimen compaction. (**b**) CBR testing

3.3. Resilient Modulus Test

The granular mixture materials are plastic, not elastic. They present different levels of permanent deformation after every mechanical load. However, when a load is small compared to the strength of the material, the deformation under the load is almost completely recoverable and presents a proportional trend with the applied load. Within this range of the load, the materials are considered elastic. The resilient modulus (Mr) may be estimated directly from laboratory testing, either indirectly through correlation with other laboratory/field tests or directly by calculation based on deflection measurements. The Mr of the mixes in this study was tested according to AASHTO T 307. Three cylindrical specimens (152 mm in diameter and 305 mm in height) were prepared for each mixture. The specimens were prepared following the same procedure of the compaction as that for the moisture–density and CBR tests, but for six different layers, each 50 mm high, that were loaded in the molds and compacted. After compaction, the prepared specimens were demolded and protected using a rubber membrane to prevent moisture loss.

Triaxial testing following AASHTO T 307 was performed to measure the Mr. Samples were loaded in a cylindric cell under a static confining stress applied through compressed air while a cyclic axial load was applied on the top of the head of samples using a pneumatic repeated loading system. To obtain the Mr, conditioning stress was applied to each specimen during 500–1000 cycles with a confining pressure (σ_c) and axial stress of 103.4 KPa, which is equivalent to a constant axial loading of 10.3 KPa plus a 93.1 cyclic axial loading. The cyclic loading consisted of a 0.1 sec loading time and 0.9 sec rest time, i.e., a 1-Hz frequency. Afterward, a series of loading cycles were applied in different sequences of confining stress and deviator stress (σ_c and σ_d) as presented in AASHTO T 307. The measured Mr is defined as the ratio of the applied deviatoric stress divided by the resilient strain for the last five cycles in each loading sequence. Figure 5 shows the triaxial test for Mr.

Figure 5. Triaxial test for resilient modulus.

4. Results and Discussion

4.1. Optimum Moisture Content (OMC %)

Figure 6 shows the optimum moisture content for the different mixtures using TTB RCA to replace the corresponding particles of the control mix CGSM. It shows that the OMC increased with the increase in the content RCA. The fine RCA particles in general

presented the highest OMC. This may be due to a combined high value of the porosity and specific particle surface area. The rate of increase in the optimum moisture content was calculated for each 25% replacement of RCA and was 0.026%, 0.471%, and 0.373% for coarse, fine, and extra fine RCA replacement, respectively.

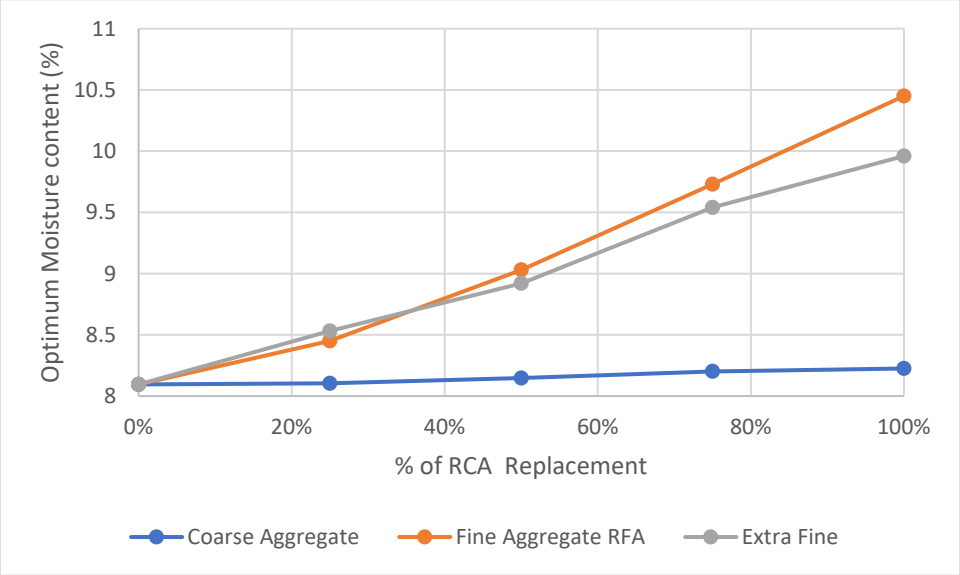

Figure 6. Optimum moisture content for the TTB RCA-replaced mixtures.

4.2. Density and CBR

Figure 7 compares the density and CBR of the mixes with coarse aggregate replacement only at the optimum moisture content. The results show that the use of RCA will reduce the density but increase the CBR magnitude in a very clear manner. It can also be seen that the CC RCA outperformed the TTB RCA to generally make the mixes lighter in weight and stronger for load bearing, particularly at the replacement rate of 25–75%. This was mostly attributed to the fact that the RCA coarse particles had a lower density but a greater strength compared with those of the virgin aggregate. This was further justified by the comparison between the mixes using TTB RCA and CC RCA at the same rate.

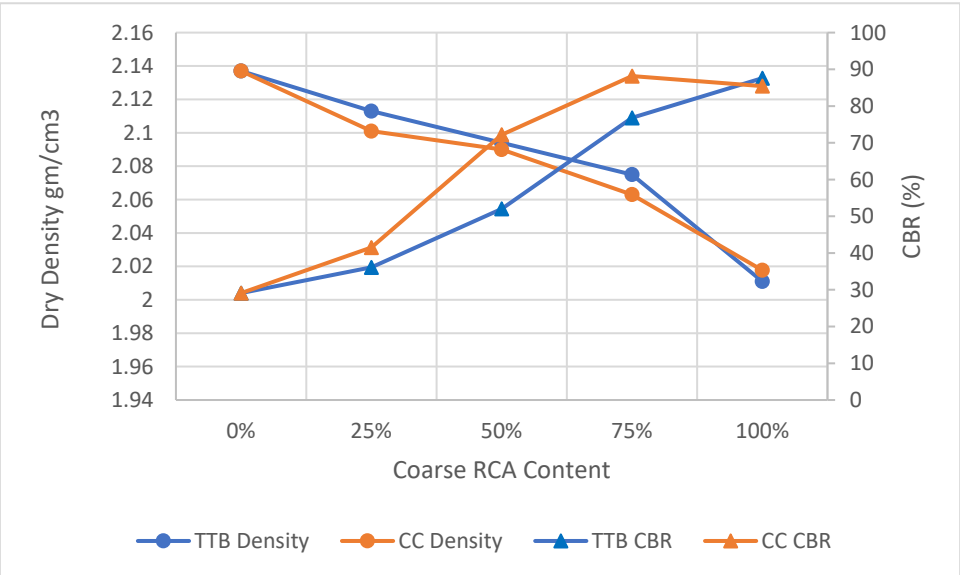

Figure 7. The effect of coarse RCA replacement on the density and CBR value.

Figure 8 compares the density and CBR of the mixes using RCA to replace the fine aggregate only. It can be seen that the effect on the density was similar to that of the coarse aggregate replacement only. The density decreased with the rate of use of RCA. In general, the use of RCA increased the CBR, but there was an optimum rate for the replacement, i.e., 50%, where the CBR achieved the highest magnitude. This may be explained as follows: the RCA fine particles, which interface between the coarse aggregate particles, decrease the cohesion of the coarse aggregates and facilitate the relative displacement of particles, reducing the stability of the mixes. A comparison of the two RCAs indicated that CC performed better than TTB in general.

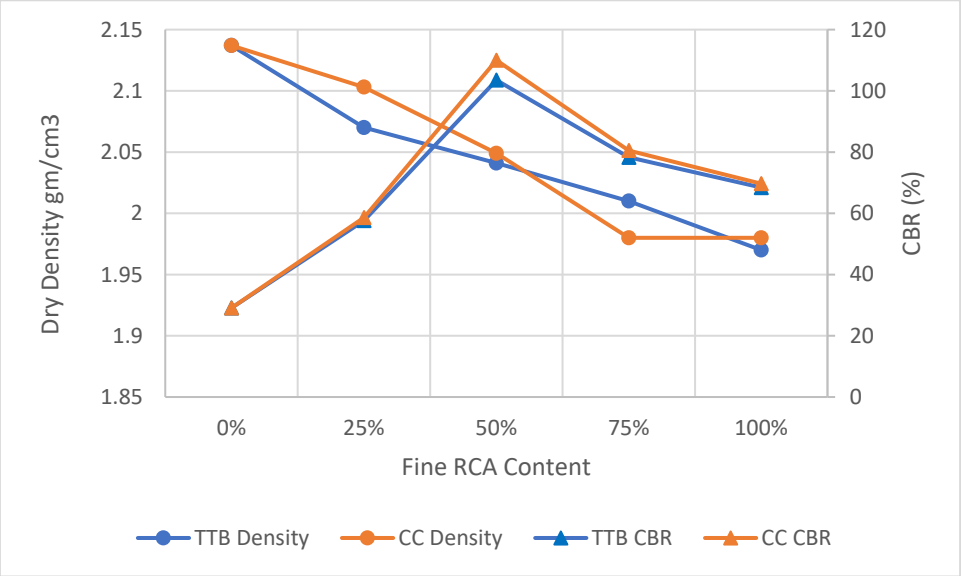

Figure 8. The effect of fine RCA replacement on the dry density and CBR value.

Figure 9 shows the results of the extra fine particle replacement only. Clear improvement for the CBR can be observed, which increased with the replacement rate, but the density of the mixes decreased. The significant effect may be explained by to the pozzolanic effect of the extra fine RCA particles, which react with the hydrated lime to reinforce the mixes. The CC RCA had a more pronounced benefit than the TTB RCA.

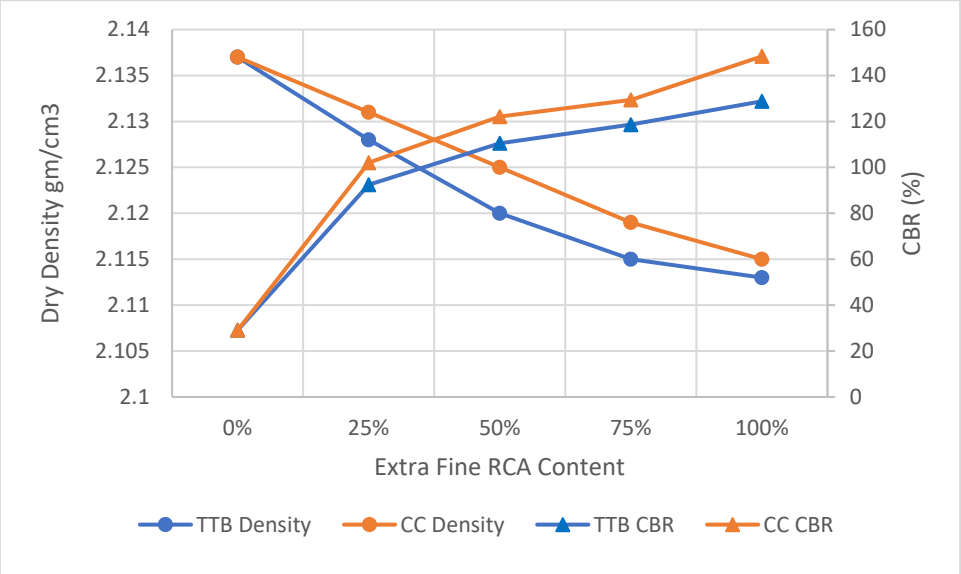

Figure 9. The effect of extra fine RCA replacement on the dry density and CBR value.

4.3. Resilient Modulus

Figures 10–12 show the results of the resilient modulus of the mixes using TTB RCA in comparison with the CGSM (CM). It can be seen that the replacement of coarse aggregates and extra fine aggregates improved the Mr, and the improvement steadily increased with the replacement rate and the level of the stress invariant. However, for the fine aggregates, the 25% replacement resulted in a lower Mr than that of the CM when the stress invariant was lower than 250 kPa. The result is in line with that observed in the density and CBR tests.

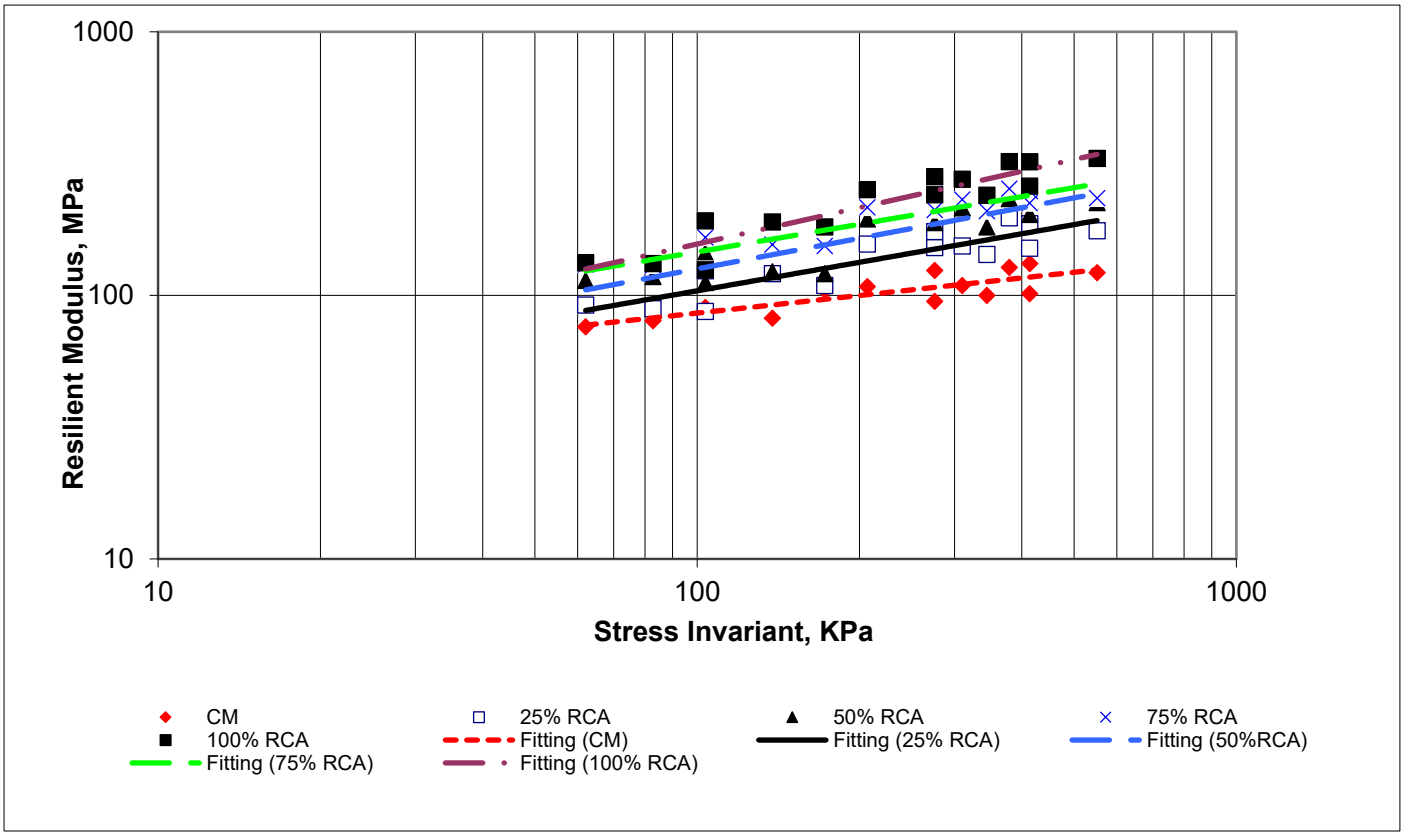

Figure 10. Resilient modulus test results obtained when using TTB RCA.

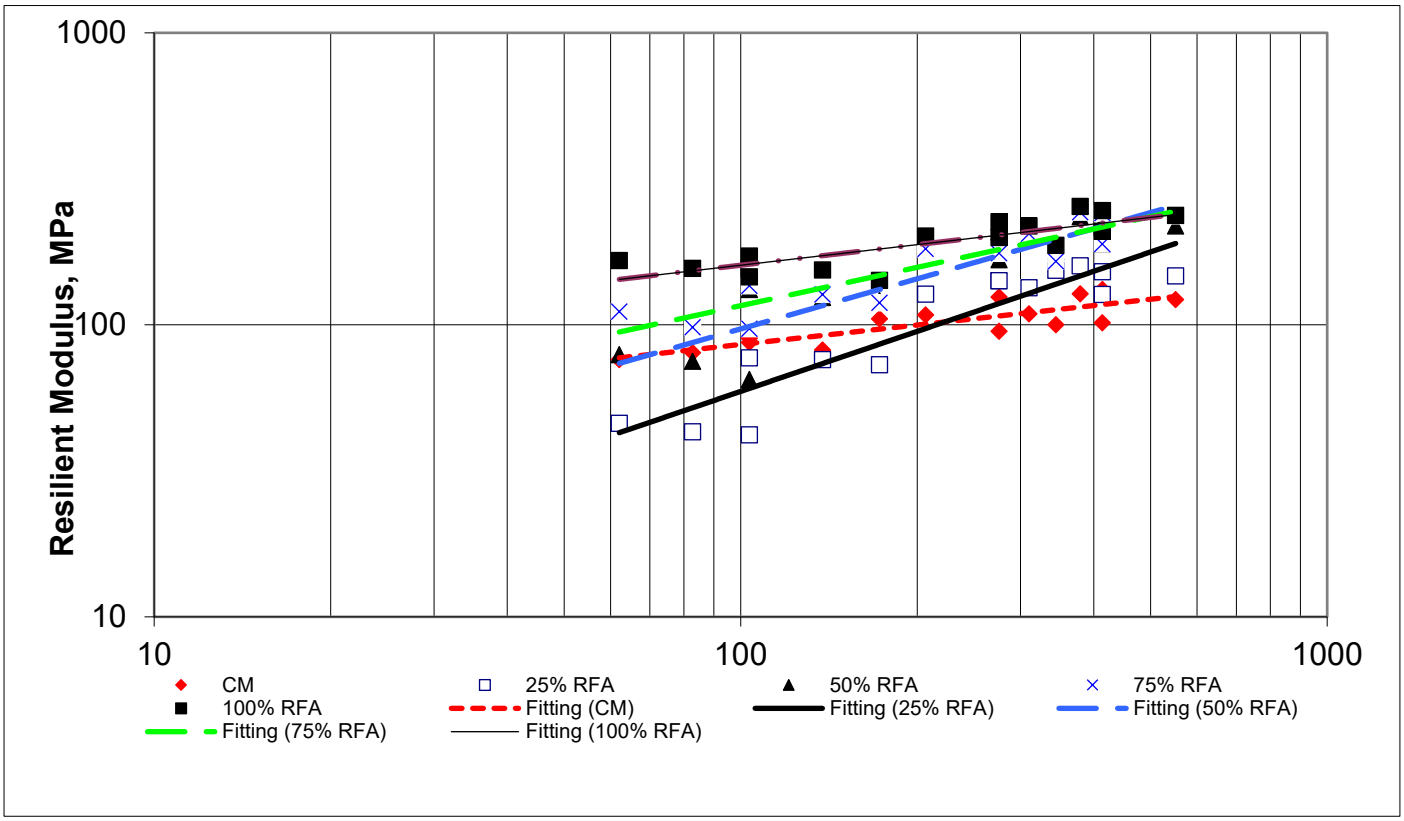

Figure 11. Resilient modulus test results obtained when using TTB RFA.

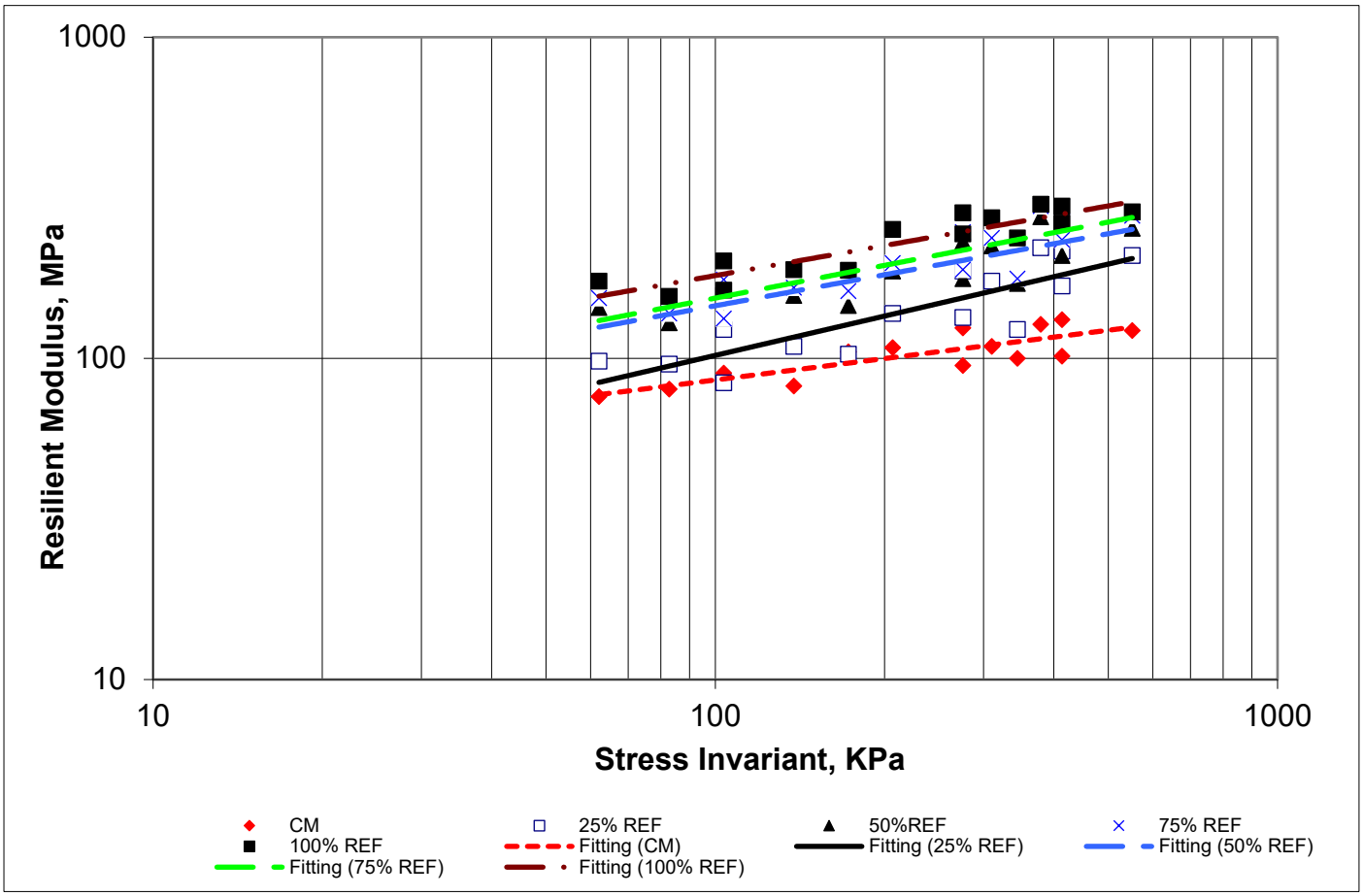

Figure 12. Resilient modulus test results obtained when using TTB REF.

Figures 13–15 show the results of the resilient modulus of the mixes using CC RCA in comparison with the CGSM (CM). A similar result was observed for the mixes using TTB RCA at three different particle size ranges. However, for the fine particle replacement, with the use of CC RCA, the replacement rate of 25% resulted in lower Mr compared to the CM when the stress invariant was lower than about 350 kPa. This could be because the CC particles with a fine size had a pronounced influence on the particle cohesion of the whole mix.

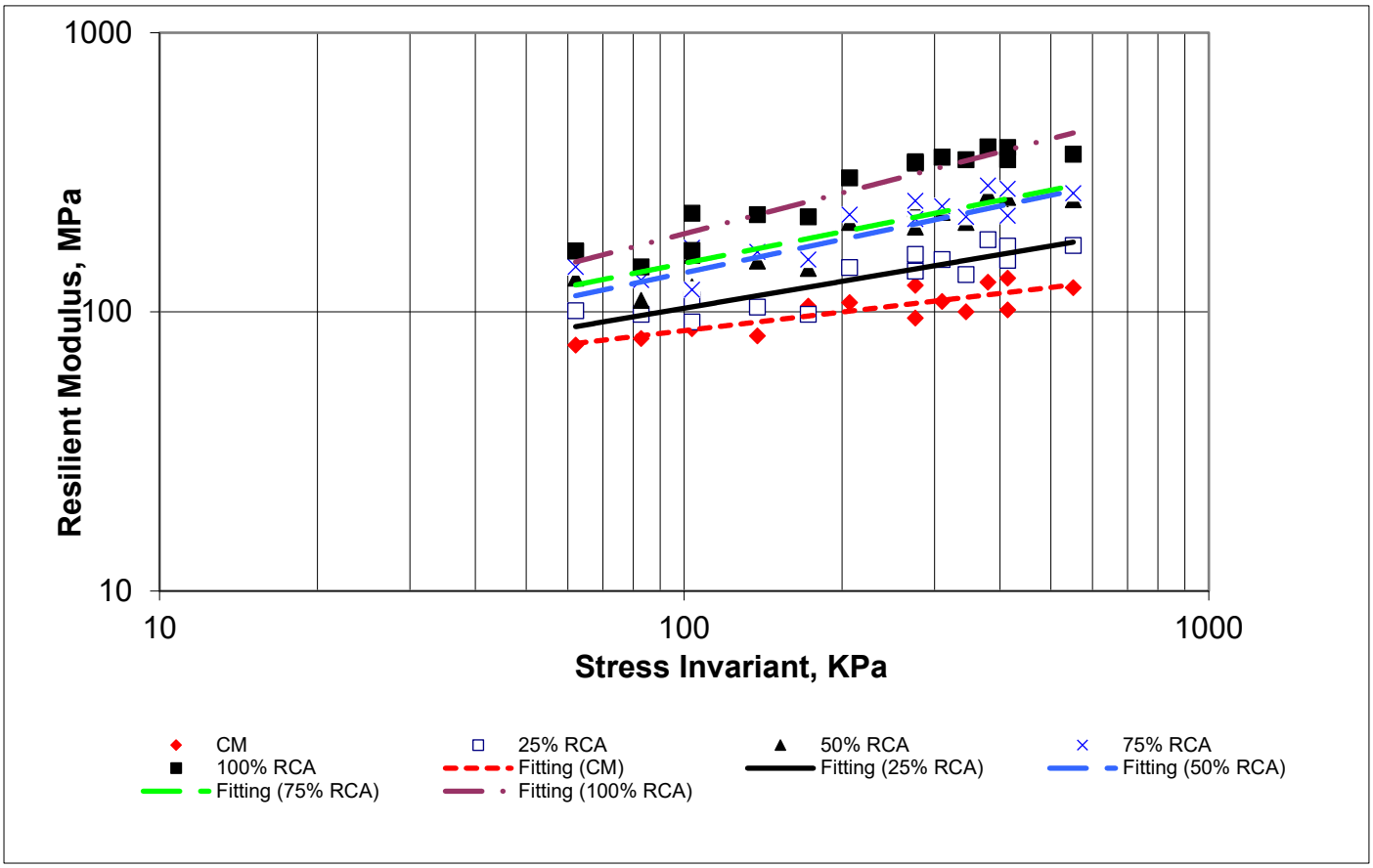

Figure 13. Resilient modulus test results obtained when using CC RCA.

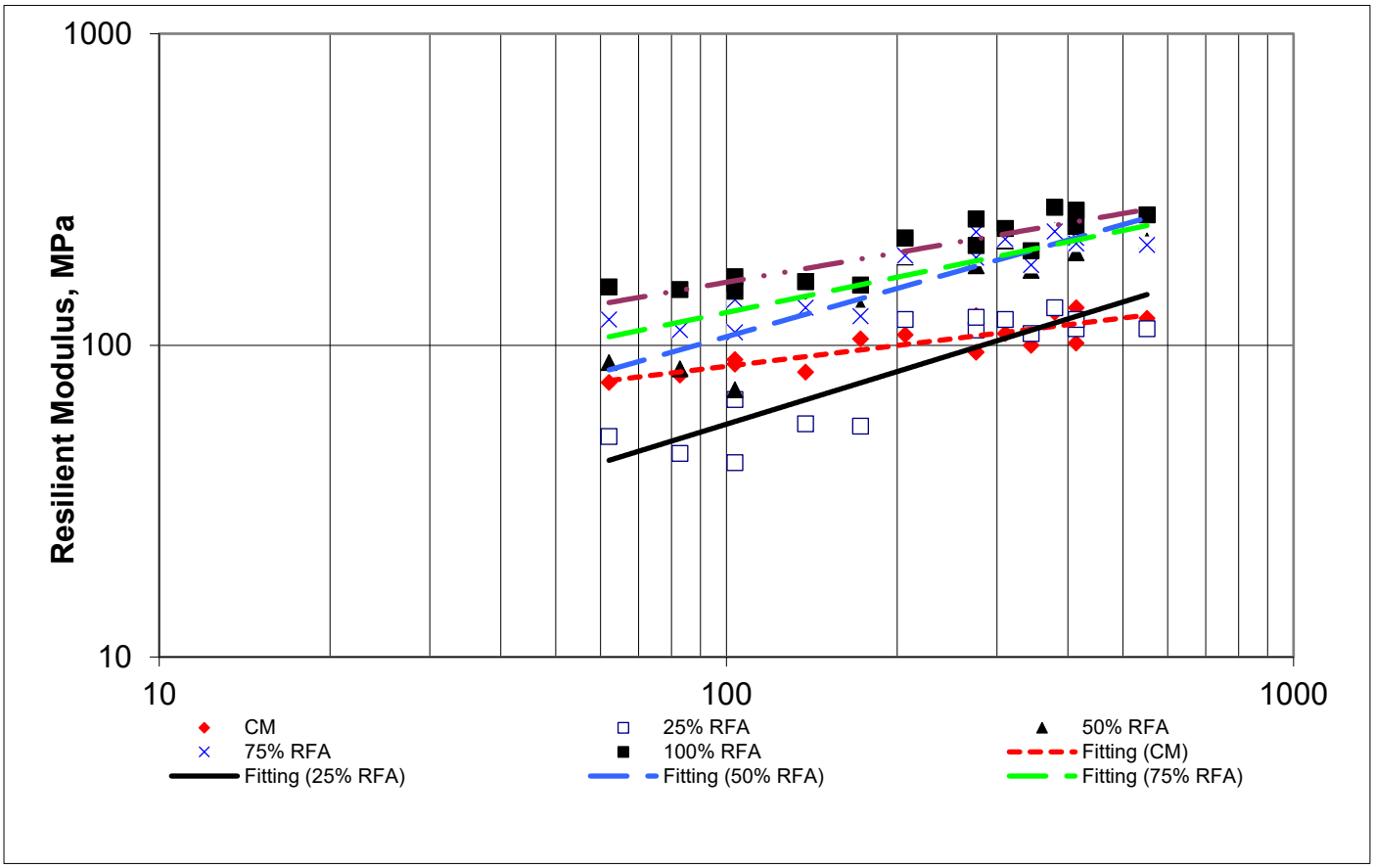

Figure 14. Resilient modulus test results obtained when using CC RFA.

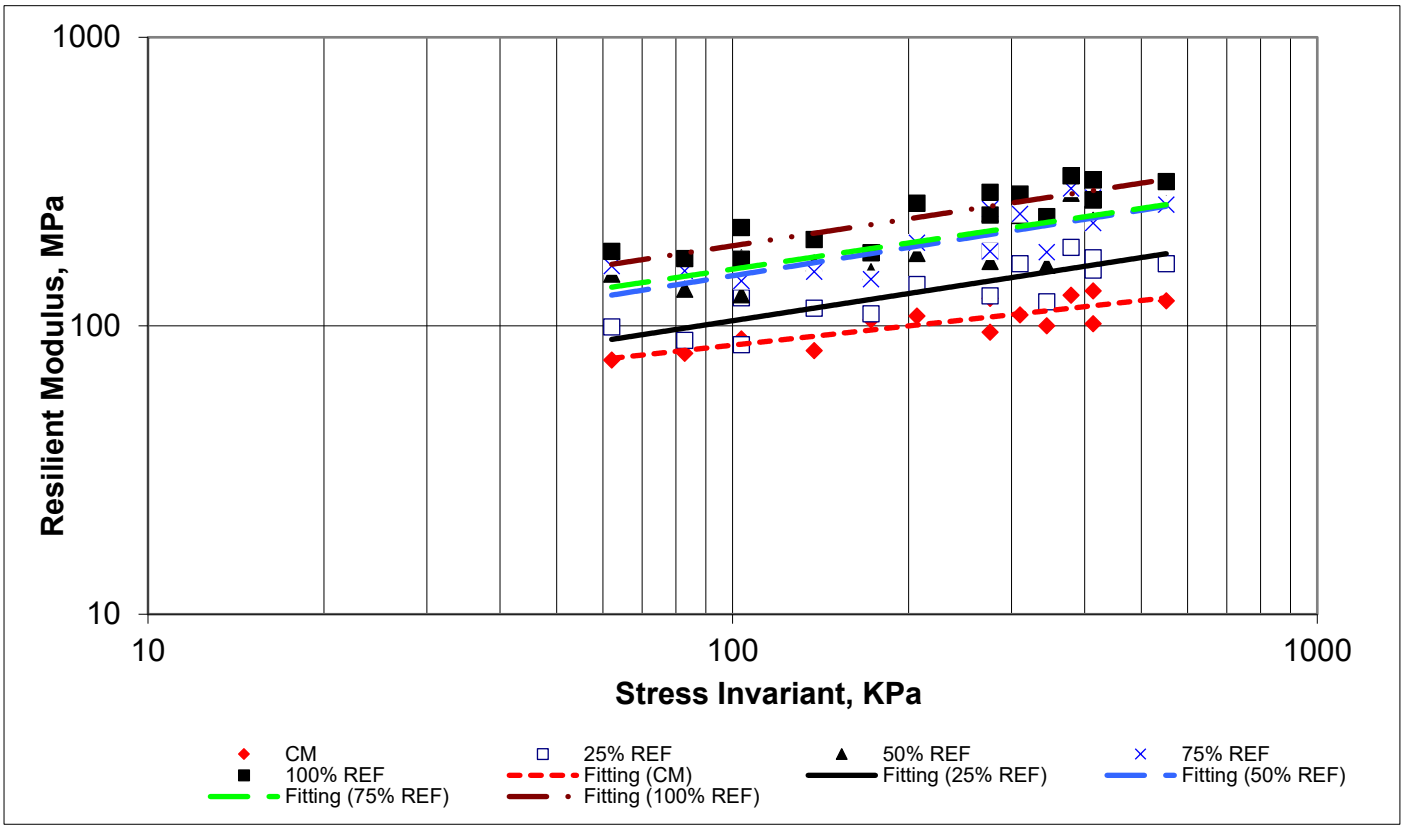

Figure 15. Resilient modulus test results obtained when using CC REF.

The above test results were characterized using a power function, Equation (1) below. Figure 16 presents the variation of the parameters, k_1 and k_2, when Equation (1) fit the Mr measurements against the stress invariant, σ. The variation of k_1 and k_2 with respect to the RCA replacement was further characterized using a quadratic function as presented in Table 3.

$$M_r = k_1 \sigma^{k_2} \quad (1)$$

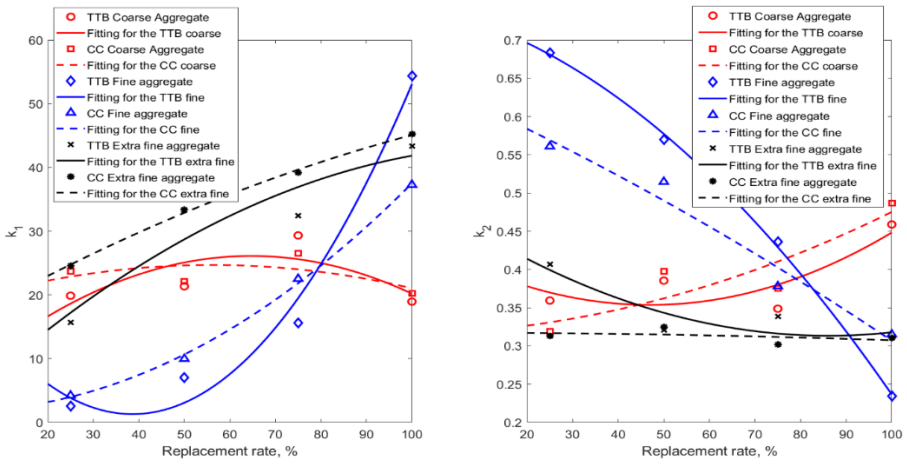

Figure 16. The variation of k_1 and k_2 with the replacement rate.

Table 3. The quadratic functions for k_1 and k_2.

	k_1	k_2
TTB_RCA	$-4.75 \times 10^{-3}x^2 + 0.61x + 6.24$	$3.36e \times 10^{-5}x^2 - 3.16 \times 10^{-3}x + 4.28 \times 10^{-1}$
CC_RCA	$-1.89 \times 10^{-3}x^2 + 0.21x + 18.76$	$1.34 \times 10^{-5}x^2 + 2.50 \times 10^{-4}x + 3.16 \times 10^{-1}$
TTB_RFA	$1.37 \times 10^{-2}x^2 - 1.06x + 21.78$	$-3.56 \times 10^{-5}x^2 - 1.48 \times 10^{-3}x + 7.4 \times 10^{-1}$
CC_RFA	$3.60 \times 10^{-2}x^2 - 3.40 \times 10^{-3}x + 1.82$	$-6.68 \times 10^{-6}x^2 - 2.66 \times 10^{-3}\ x + 6.4 \times 10^{-1}$
TTB_EFA	$-2.64 \times 10^{-3}x^2 + 6.59 \times 10^{-1}x + 2.39$	$2.30 \times 10^{-5}x^2 - 3.97 \times 10^{-3}x + 4.84 \times 10^{-1}$
CC_EFA	$-1.08 \times 10^{-3}x^2 + 4.06 \times 10^{-1}x + 15.3$	$-1.0 \times 10^{-6}x^2 + 6.0 \times 10^{-7}x + 3.17 \times 10^{-1}$

4.4. Non-Linear Pavement Analysis

The Mr characterized by Equation (1) and k_1 and k_2 in Table 3 were used to analyze a three-layered pavement structure using the modelling tool KENLAYER. In total, 26 modeling cases were performed to compute the elastic deformation of the constructed pavement structure using the different mixes of degree usages of the RCA for the subbase course. The analysis assumed a variation in the vertical direction (depth) according to the material properties. The pavement structure had one asphaltic layer with a thickness of 101.6 mm (4 in.) on the top of the subbase course with 12 layers. Each of the subbase courses was 25.4 mm (1 in.) thick and consisted of the materials studied above as shown in Figure 17. The tensile strain at the bottom of the asphalt layer and the vertical compressive strain at the top of the subgrade were computed and compared.

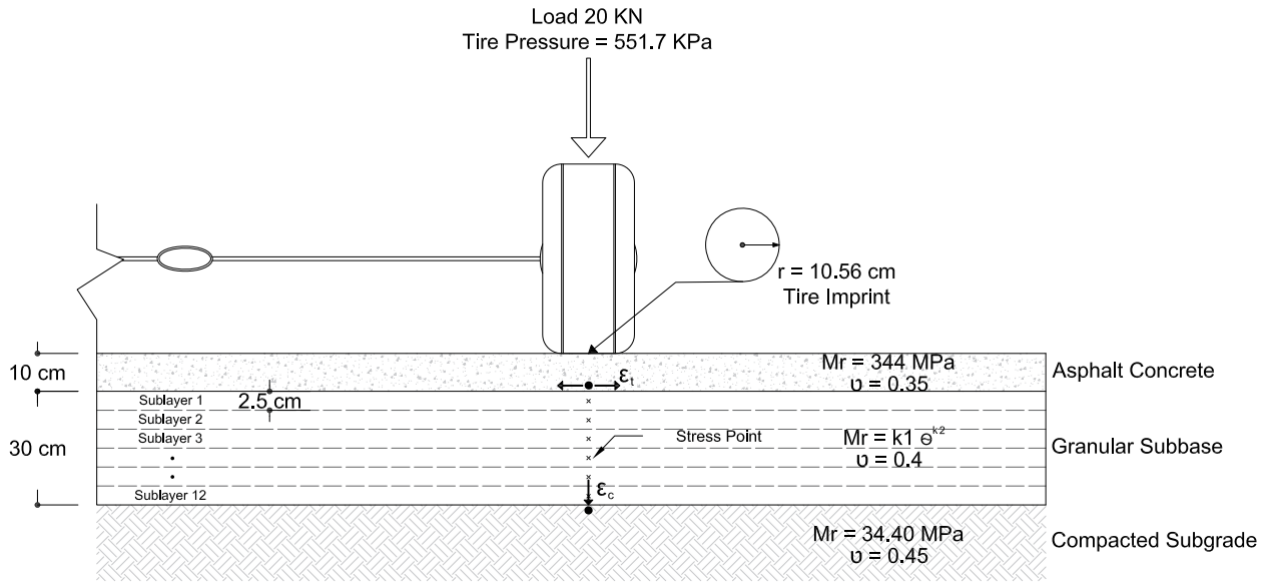

Figure 17. Pavement structure model with loading configuration.

Figures 18–21 shows the behavior of the critical responses of the pavement when different replacement types and percentages were used. It can be observed that the addition of recycled concrete aggregate to the subbase resulted in a noticeable decrease in the compressive and tensile strain due to the increase in the resilient modulus. In the same manner, the critical tensile strain also decreased with the increase in the RCA. For all of the pavement responses shown in Figures 16–19, the 25% RFA addition to the subbase material had a negative effect on the behavior of the subbase. However, at high stress levels, these mixtures had high Mr values as shown in Figures 11 and 14.

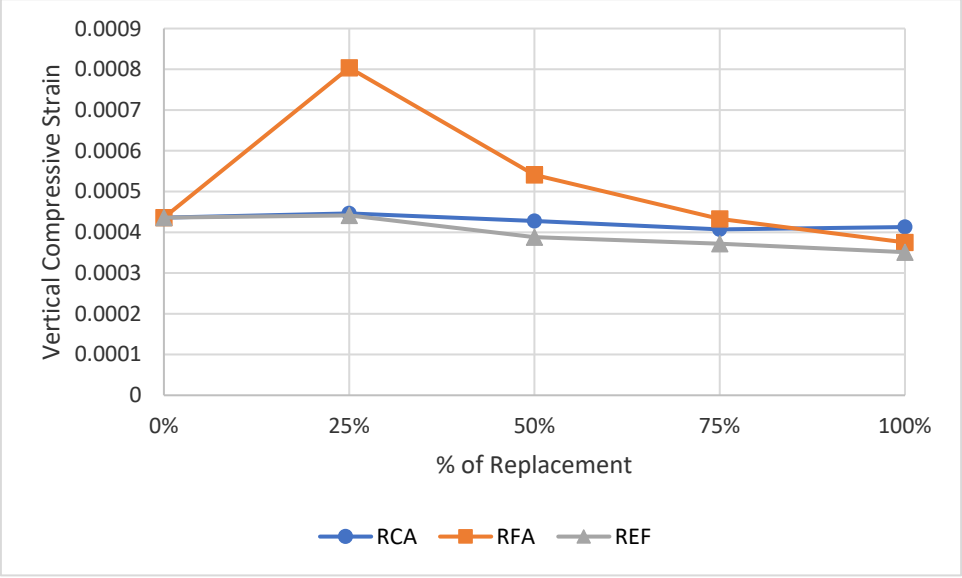

Figure 18. Vertical compressive strain for the modified subbase with CC RCA.

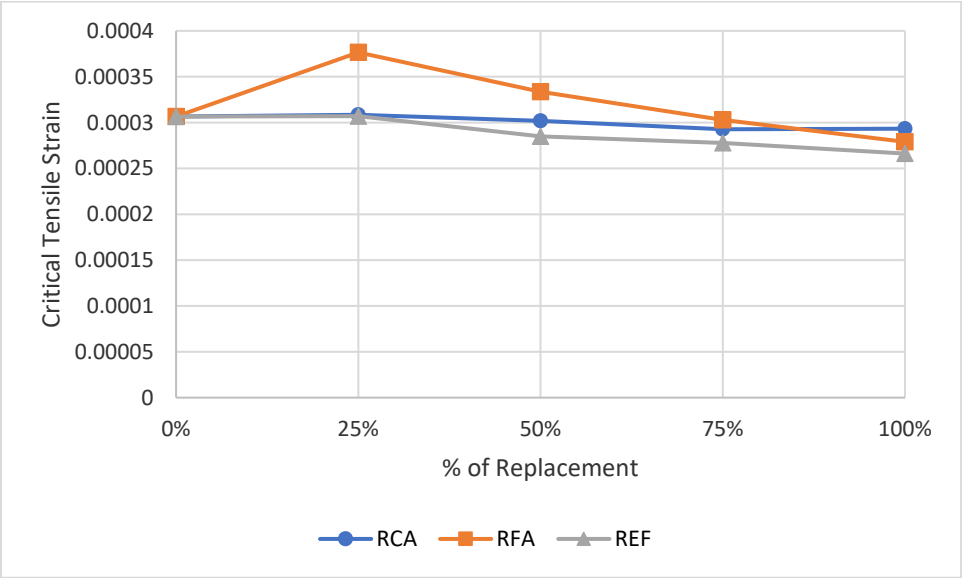

Figure 19. Critical tensile strain for the modified subbase with CC RCA.

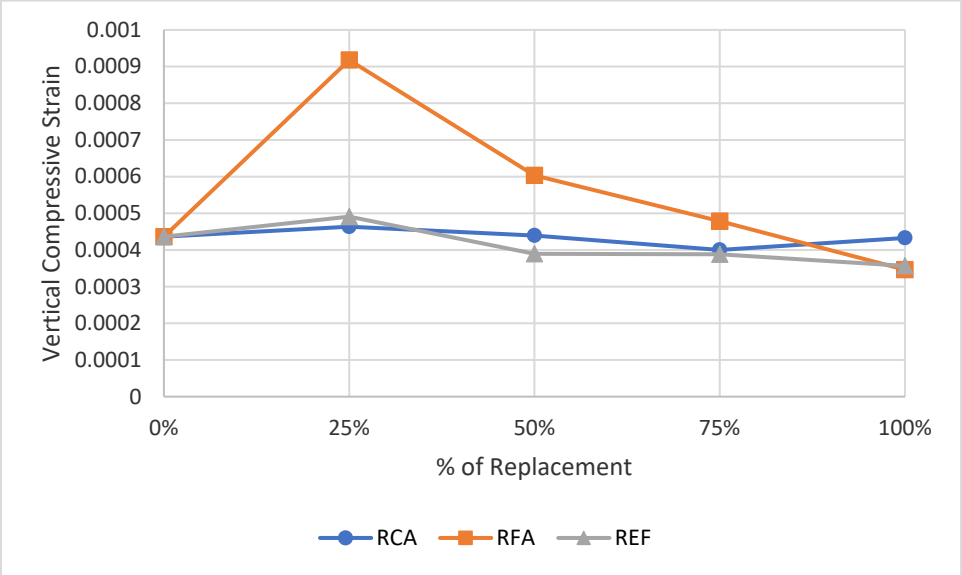

Figure 20. Vertical compressive strain for the modified subbase with TTB RCA.

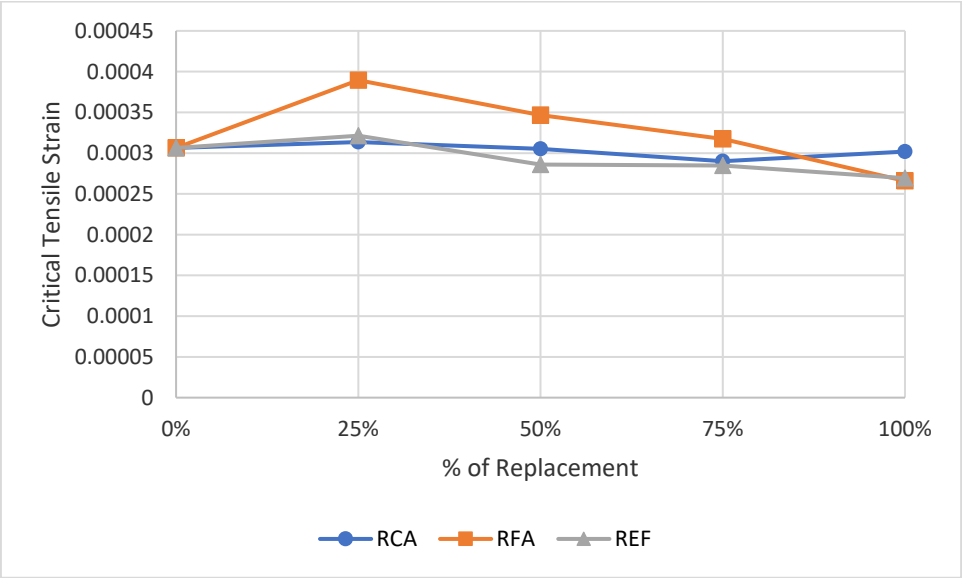

Figure 21. Critical tensile strain for the modified subbase with TTB RCA.

Figures 22 and 23 shows the vertical profile of the resilient modulus inside the pavement structure. It can be observed that the replacement of 25% RFA had the least modulus variation along the pavement depth direction for both TTB and CC RCA. However, the use of 100% CC RCA for the extra-fine aggregates resulted in the highest rigidness at all depths, particularly on the top surface of the pavement. With the use of the TTB RCA, the highest rigidness was obtained with 100% replacement of the fine aggregates, also at the surface. Meanwhile, both results showed that the vertical resilient modulus decreased with depth, and the trend steadily increased with the improvement in the total average rigidity of the whole pavement structure.

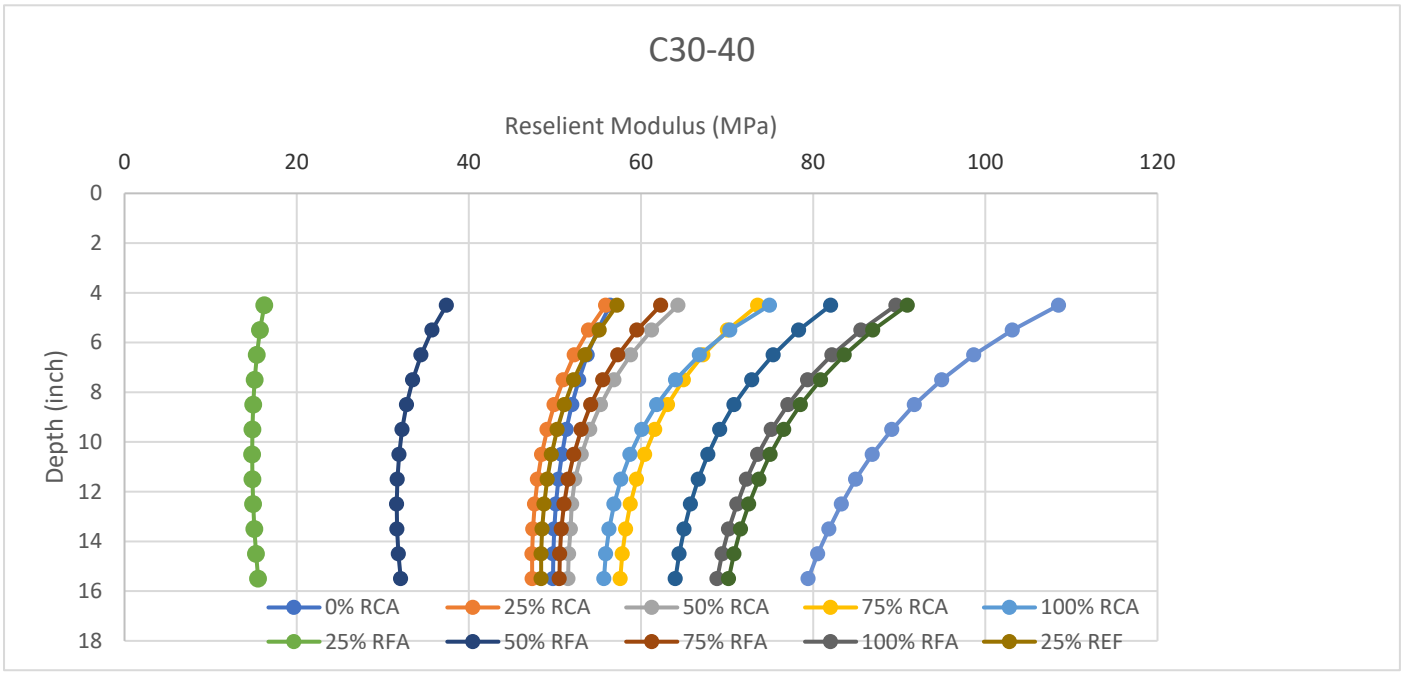

Figure 22. Mr variation with depth for the modified subbase with CC RCA.

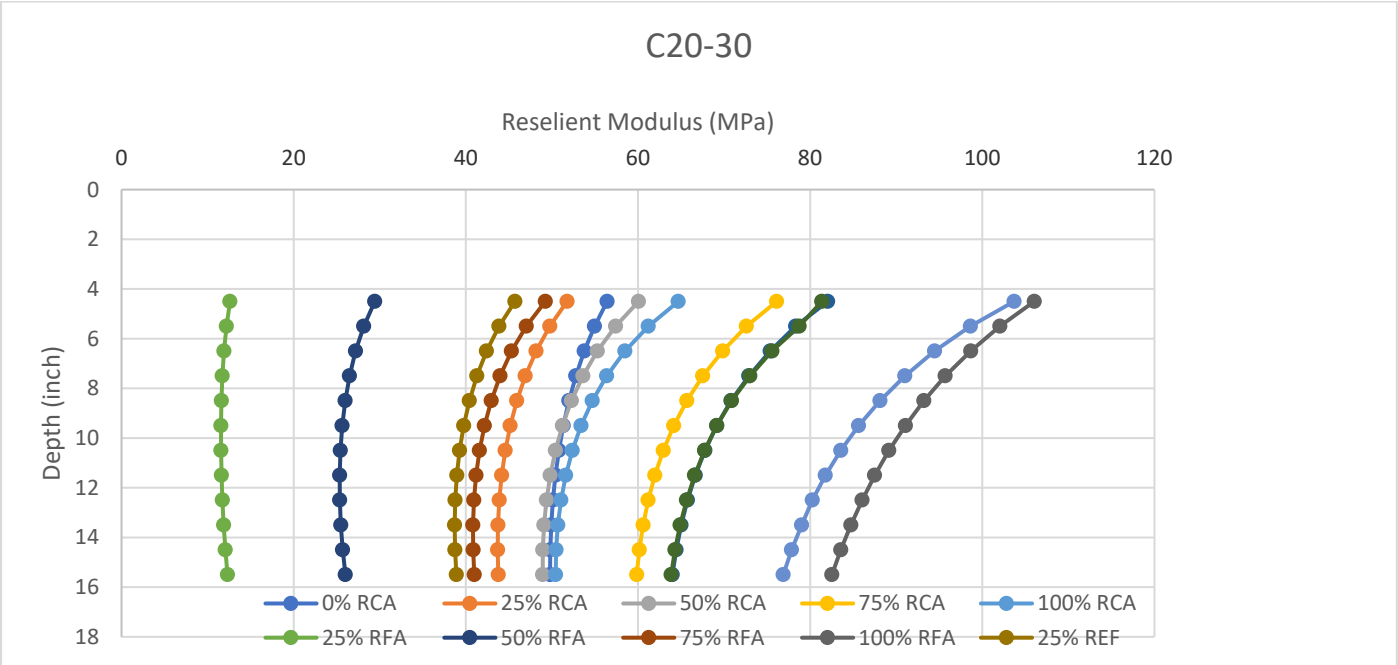

Figure 23. Mr variation with depth for the modified subbase with TTB RCA.

SEM images were taken of the VA and RCA particles, as shown in Figure 24. The VA SEM image contained crystals of different sizes and morphologies. Generally, many small crystals were visible in the particles, having the appearance of fragments obtained by the destruction of large crystals. The contact between the individual crystals was weak. This indicates the absence of chemical reactions between them. The RCA particles were shell-like grains, and they were produced during the chemical reaction that produced the concrete; therefore, the environment was heterogeneous. The particles had more angular edges, and pores were created between large particles, which allowed interlocking to occur. Generally, a higher grey scale in SEM images indicates a higher density of the material discovered; in this case, the VA particles were more dense then the RCA particles.

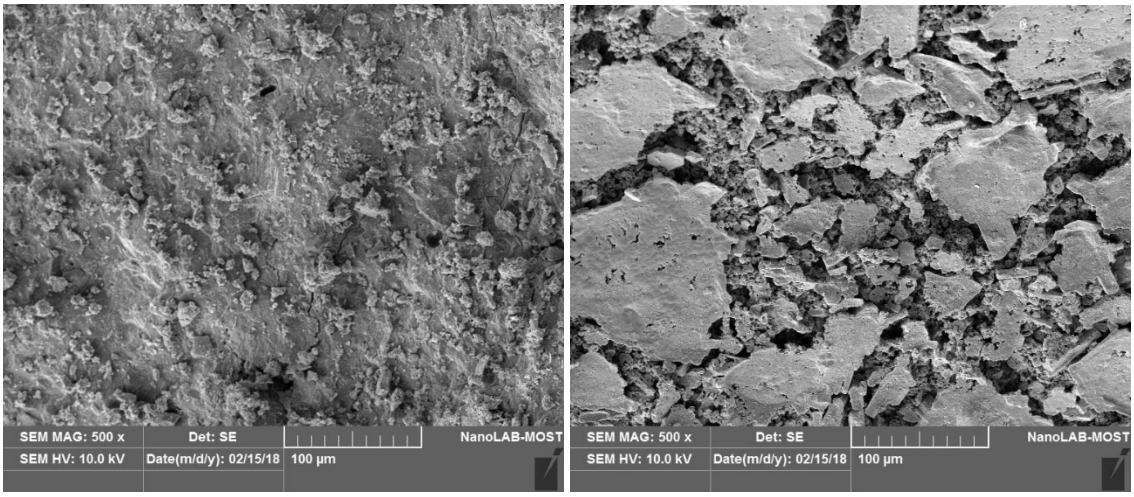

(**a**) (**b**)

Figure 24. (**a**) VA SEM image; (**b**) RCA SEM image.

5. Conclusions

The use of recycled materials is increasingly adopted by researchers using different types of waste materials aiming to produce a newly eco-friendly sustainable construction

material. This study used recycled concrete materials to enhance the properties of the pavement roadbed materials. From the experimental study and modelling of this work, the following three conclusions were drawn:

- RCA can be used to replace ordinary gravel materials at full scale to meet the requirement for pavement subbase layer construction in terms of the material specification.
- RCA materials have a higher optimum moisture content in comparison with ordinary gravel material. If linearity is implied, the constant proportions would be 0.026%, 0.471%, and 0.373% for the coarse, fine, and extra fine materials, respectively.
- In general, using RCA to replace the ordinary gravel material for subbase course construction will enhance the bearing capacity and rigidness of the whole pavement structure, and the benefit would be particularly pronounced in the pavement surface layer with asphalt.
- The optimum use of replacement to obtain a higher CBR value was achieved by using 75% coarse RCA replacement, 50% fine RCA replacement, or 100% extra fine replacement.
- The 100% REF replacement minimized the critical tensile strain and maximum compressive strain when using the CC RCA type. On the other hand, the 100% RFA replacement enhanced these two parameters when using the TTB RCA type. These two recommended replacements also maximized the value of the resilient modulus.
- The use of the proposed replacement would cause the number of allowable load repetitions to increase, resulting in a longer design life of the pavement structure.

Author Contributions: Conceptualization, A.A.; methodology, A.A.; software, H.A.-M.; validation, Y.W.; formal analysis, H.A.-M.; investigation, N.S.M.; resources, A.A.; data curation, H.A.-M.; writing— original draft preparation, A.A.; writing—review and editing, Y.W. and H.A.-M.; visualization, N.S.M.; supervision, A.A.; project administration, H.A.-M. All authors have read and agreed to the published version of the manuscript.

Funding: This research received no external funding.

Institutional Review Board Statement: Not applicable.

Informed Consent Statement: Not applicable.

Data Availability Statement: Not applicable.

Conflicts of Interest: The authors declare no conflict of interest.

References

1. Stone Cycling, 2021, 28 Incredible Statistics About Waste Generation: Global, US, UK & European Union. Available online: https://www.stonecycling.com/news/statistics-about-waste-generation/ (accessed on 14 September 2022).
2. Kaza, S.; Yao, L.; Bhada-Tata, P.; Van Woerden, F. *What a Waste 2.0: A Global Snapshot of Solid Waste Management to 2050*; The World Bank: Washington, DC, USA, 2018. Available online: https://datatopics.worldbank.org/what-a-waste/ (accessed on 21 September 2022).
3. Karalar, M.; Özkılıç, Y.O.; Deifalla, A.F.; Aksoylu, C.; Arslan, M.H.; Ahmad, M.; Sabri, M.M.S. Improvement in Bending Performance of Reinforced Concrete Beams Produced with Waste Lathe Scraps. *Sustainability* **2022**, *14*, 12660.
4. Aksoylu, C.; Özkılıç, Y.O.; Hadzima-Nyarko, M.; Işık, E.; Arslan, M.H. Investigation on Improvement in Shear Performance of Reinforced-Concrete Beams Produced with Recycled Steel Wires from Waste Tires. *Sustainability* **2022**, *14*, 13360.
5. Çelik, A.İ.; Özkılıç, Y.O.; Zeybek, Ö.; Özdöner, N.; Tayeh, B.A. Performance Assessment of Fiber-Reinforced Concrete Produced with Waste Lathe Fibers. *Sustainability* **2022**, *14*, 11817.
6. Qaidi, S.; Najm, H.M.; Abed, S.M.; Özkılıç, Y.O.; Al Dughaishi, H.; Alosta, M.; Sabri, M.M.S.; Alkhatib, F.; Milad, A. Concrete Containing Waste Glass as an Environmentally Friendly Aggregate: A Review on Fresh and Mechanical Characteristics. *Materials* 2022, *15*, 6222.
7. Özkılıç, Y.O.; Karalar, M.; Bilir, T.; Çavuşli, M.; Sabri, M. Use of Recycled Coal Bottom Ash in Reinforced Concrete Beams as Replacement for Aggregate. *Frontiers in Materials* 675, *in press*. Available online: https://www.frontiersin.org/articles/10.3389/fmats.2022.1064604/abstract (accessed on 21 September 2022)
8. Tam, V.W. Economic comparison of concrete recycling: A case study approach. *Resour. Conserv. Recycl.* **2008**, *52*, 821–828.

9. Arabani, M.; Azarhoosh, A.R. The effect of recycled concrete aggregate and steel slag on the dynamic properties of asphalt mixtures. *Constr. Build. Mater.* **2012**, *35*, 1–7.
10. Marinković, S.B.; Ignjatović, I.S.; Radonjanin, V.S.; Malešev, M.M. Recycled aggregate concrete for structural use—An overview of technologies, properties and applications. *Conf. Proc. —Innov. Mater. Tech. Concr. Constr.* **2012**, 115–130.
11. Pourkhorshidi, S.; Sangiorgi, C.; Torreggiani, D.; Tassinar, P. Using Recycled Aggregates from Construction and DemolitionWaste in Unbound Layers of Pavements. *Sustainability* **2020**, *12*, 9386. https://doi.org/10.3390/su12229386.
12. Shi, C.; Li, Y.; Zhang, J.; Li, W.; Chong, L.; Xie, Z. Performance enhancement of recycled concrete aggregate–a review. *J. Clean. Prod.* **2016**, *112*, 466–472.
13. Courard, L.; Michel, F.; Delhez, P. Use of concrete road recycled aggregates for roller compacted concrete. *Constr. Build. Mater.* **2010**, *24*, 390–395.
14. Li, Y.; Zhou, Y.; Wang, R.; Li, Y.; Wu, X.; Si, Z. Experimental investigation on the properties of the interface between RCC layers subjected to early-age frost damage. *Cem. Concr. Compos.* **2022**, *134*, 104745.
15. Seferoğlu, A.G.; Seferoğlu, M.T.; Akpınar, M.V. Investigation of the effect of recycled asphalt pavement material on permeability and bearing capacity in the base layer. *Adv. Civ. Eng.* **2018**, *2018*.
16. Toka, E.B.; Olgun, M. Performance of granular road base and sub-base layers containing recycled concrete aggregate in different ratios. *Int. J. Pavement Eng.* **2021**, 1–14. https://doi.org/10.1080/10298436.2021.1916819.
17. Tran, D.V.P.; Allawi, A.; Albayati, A.; Cao, T.N.; El-Zohairy, A.; Nguyen, Y.T.H. Recycled concrete aggregate for medium-quality structural concrete. *Materials* **2021**, *14*, 4612.
18. Alnedawi, A.; Md, A.R. Recycled concrete aggregate as alternative pavement materials: Experimental and parametric study. *J. Transp. Eng. Part B Pavements* **2021**, *147*, 04020076.
19. Farhan, O.S. Effect of Use Recycled Coarse Aggregate on the Behavior of Axially Loaded Reinforced Concrete Columns. *J. Eng.* **2019**, *25*, 88–107.
20. Albayati, A.H.; Al-Mosawe, H.M.; Allawi, A.A.; Oukaili, N. Moisture susceptibility of sustainable warm mix asphalt. *Adv. Civ. Eng.* **2018**, *2018*, 1-9.
21. Albayati, A.; Wang, Y.; Wang, Y.; Haynes, J. A sustainable pavement concrete using warm mix asphalt and hydrated lime treated recycled concrete aggregates. *Sustain. Mater. Technol.* **2018**, *18*, e00081.
22. Hama, S.M.; Hama, S.M.; Mhana, M.H. Improving Strengths of Porcelanite Aggregate Concrete by Adding Chopped Carbon Fibers. *Al-Nahrain J. Eng. Sci.* **2018**, *21*, 161–165.
23. Haynes, J.H. Effects of repeated loading on gravel and crushed stone base course materials used in the AASHO Road Test, Purdue University, Report **1963**.
24. Barksdale, R.D. Laboratory evaluation of rutting in base course materials. In Proceedings of the Third International Conference on the Structural Design of Asphalt Pavements, Grosvenor House, Park Lane, London, UK, 11–15 September 1972.
25. Lekarp, F.; Isacsson, U.; Dawson, A. State of the art. II: Permanent strain response of unbound aggregates. *J. Transp. Eng.* **2000**, *126*, 76–83.
26. Abid, A.N.; Salih, A.O.; Nawaf, E.A. The influence of fines content on the mechanical properties of aggregate subbase course material for highway construction using repeated load CBR test. *Al-Nahrain J. Eng. Sci.* **2017**, *20*, 615–624.
27. Poon, C.S.; Chan, D. Feasible use of recycled concrete aggregates and crushed clay brick as unbound road sub-base. *Constr. Build. Mater.* **2006**, *20*, 578–585.
28. Dunlap, W.A. *Deformation Characteristics of Granular Materials Subjected to Rapid, Repetitive Loading*; Texas A&M University: College Station, TX, USA, 1966.
29. Thai, H.N.; Nguyen, T.D., Nguyen, V.T.; Nguyen, H.G.; Kawamoto, K. Characterization of compaction and CBR properties of recycled concrete aggregates for unbound road base and subbase materials in Vietnam. *J. Mater. Cycles Waste Manag.* **2022**, *24*, 34–48.
30. Signes, C.H.; Fernández, P.M.; Garzón-Roca, J.; de la Torre, M.E.G.; Franco, R.I. An evaluation of the resilient modulus and permanent deformation of unbound mixtures of granular materials and rubber particles from scrap tyres to be used in subballast layers. *Transp. Res. Procedia* **2016**, *18*, 384–391.